



***Free-Flow Zone Electrophoresis of Peptides and Proteins  
in PDMS Microchip for Narrow pI Range Sample  
Prefractionation Coupled with Mass Spectrometry***

The MIT Faculty has made this article openly available. **Please share** how this access benefits you. Your story matters.

<b>Citation</b>	Song, Yong-Ak et al. "Free-Flow Zone Electrophoresis of Peptides and Proteins in PDMS Microchip for Narrow pI Range Sample Prefractionation Coupled with Mass Spectrometry." Analytical Chemistry 82 (2010): 2317-2325. Web. 2 Nov. 2011. © 2011 American Chemical Society
<b>As Published</b>	<a href="http://dx.doi.org/10.1021/ac9025219">http://dx.doi.org/10.1021/ac9025219</a>
<b>Publisher</b>	American Chemical Society
<b>Version</b>	Author's final manuscript
<b>Accessed</b>	Sun Jan 31 22:30:30 EST 2016
<b>Citable Link</b>	<a href="http://hdl.handle.net/1721.1/66895">http://hdl.handle.net/1721.1/66895</a>
<b>Terms of Use</b>	Creative Commons Attribution-Noncommercial-Share Alike 3.0
<b>Detailed Terms</b>	<a href="http://creativecommons.org/licenses/by-nc-sa/3.0/">http://creativecommons.org/licenses/by-nc-sa/3.0/</a>



# NIH Public Access

## Author Manuscript

*Anal Chem.* Author manuscript; available in PMC 2011 March 15.

Published in final edited form as:  
*Anal Chem.* 2010 March 15; 82(6): 2317–2325. doi:10.1021/ac9025219.

## Free-Flow Zone Electrophoresis of Peptides and Proteins in PDMS Microchip for Narrow pI Range Sample Prefractionation Coupled with Mass Spectrometry

**Yong-Ak Song<sup>1,2</sup>, Michael Chan<sup>4</sup>, Chris Celio<sup>1</sup>, Steven R. Tannenbaum<sup>2,3</sup>, John S. Wishnok<sup>2</sup>, and Jongyoon Han<sup>1,2</sup>**

<sup>1</sup>Department of Electrical Engineering and Computer Science, Massachusetts Institute of Technology, 77 Massachusetts Ave., Cambridge, MA 02139

<sup>2</sup>Department of Biological Engineering, Massachusetts Institute of Technology, 77 Massachusetts Ave., Cambridge, MA 02139

<sup>3</sup>Department of Chemistry, Massachusetts Institute of Technology, 77 Massachusetts Ave., Cambridge, MA 02139

<sup>4</sup>Department of Bioengineering, Imperial College London, Exhibition Road, London SW7 2AZ

### Abstract

In this paper, we are evaluating the strategy of sorting peptides / proteins based on the charge to mass without resorting to ampholytes and / or isoelectric focusing, using a single- and two-step free-flow zone electrophoresis. We developed a simple fabrication method to create a salt bridge for free-flow zone electrophoresis in PDMS chips by surface printing a hydrophobic layer on a glass substrate. Since the surface-printed hydrophobic layer prevents plasma bonding between the PDMS chip and the substrate, an electrical junction gap can be created for free-flow zone electrophoresis. With this device, we demonstrated a separation of positive and negative peptides and proteins at a given pH in standard buffer systems, and validated the sorting result with LC/MS. Furthermore, we coupled two sorting steps via off-chip titration, and isolated peptides within specific pI ranges from sample mixtures, where the pI range was simply set by the pH values of the buffer solutions. This free-flow zone electrophoresis sorting device, with its simplicity of fabrication, and a sorting resolution of 0.5 pH unit, can potentially be a high-throughput sample fractionation tool for targeted proteomics using LC/MS.

### Keywords

Microfluidics; sample preparation; peptide/protein separation; transverse electrophoresis; free-flow zone electrophoresis; mass spectrometry

### INTRODUCTION

One of the most widely used Mass Spectrometry (MS)-based proteomic detection techniques is MudPIT (Multidimensional Protein Identification Technology)<sup>1, 2</sup>, where strong cation-exchange chromatography (SCX) and reverse-phase liquid chromatography (RP-LC) are coupled with Electrospray Ionization(ESI)-MS. However, there are problems associated with strong cation-exchange chromatography like high-salt load and poor resolution.<sup>3</sup> In view of

this current deficit, we propose to develop an ampholyte-free, two-step cascaded microfluidic sorting technique based on free-flow zone electrophoresis that isolates the molecules of interest from a small sample volume of 100  $\mu\text{L}$  within narrow and freely adjustable pI range ( $\leq 1$  pH units), even below pH 3 and beyond pH 10. This method will allow for liquid-phase sample recovery after fractionation without using ampholytes for direct sample analysis by MS. Several approaches have already been taken to develop continuous free-flow zone electrophoresis in a microfluidic chip format.<sup>4-5</sup> The key engineering issue has been how to couple an electric field efficiently into the sorting process while creating a hydrodynamic barrier between the separation channel and the electrode channels in the form of a membrane. Microchannels<sup>6</sup>, acrylamide gels<sup>7-10</sup> and dielectric materials such as glass<sup>11</sup> have been used as membranes. Curing the gel inside the PDMS devices, however, has been challenging due to the oxygen barrier on the surface and, therefore, glass has been used as alternative material despite requirements for complex fabrication and separate masks for the polymerization of the membranes.<sup>7, 8</sup> In addition, gel membranes show limited stability under pressure-driven flow. Although an open connection between the separation channel and the reservoirs allowed the highest electric field across the separation channel<sup>12</sup>, control of the flow rate was challenging, requiring a high flow rate of the electrolytes in the side channels at 10–20  $\mu\text{L}/\text{min}$ . Recently, the same group has used channel depth variation to control the flow in a 20  $\mu\text{m}$  deep separation channel versus a 78  $\mu\text{m}$  electrode channel.<sup>13</sup> Using higher channel depth to control buffer flow over the electrodes increased the linear velocity ~15 times that of the buffer in the separation channel and removed electrolysis products for more stable separation process. A dielectric wall is another available solution for the membrane, allowing 50% of the electric field without constant flow of the electrolyte solutions. However, glass chips require wet etching steps and they are therefore more difficult to fabricate than PDMS chips.

In this paper, we are demonstrating a simple, low-cost fabrication method for free-flow zone electrophoresis device, which has been the basis of our sorting technique. To meet the requirements of an efficient coupling of the electrical field from the electrode channels to the sorting channel while offering sufficient hydrodynamic resistance, we have printed a submicron thick hydrophobic material on the glass substrate prior to plasma bonding to a PDMS chip to create controlled rupture points when applying positive pressure inside the device.<sup>14</sup> These rupture points with small openings, possibly in the range of only few micrometers or less, act as junction gaps between the sorting channel and electrode channels. With this device, we demonstrated continuous-flow separation of proteins and peptides at flow rates up to 1  $\mu\text{L}/\text{min}$  and validated the sorting result with both MALDI (Matrix-Assisted Laser Desorption/Ionization) and ESI (Electrospray Injection) mass spectrometry.

## MATERIALS AND METHODS

### Chip Fabrication

All experiments were performed in microfluidic chips made of polydimethylsiloxane (PDMS) (Sylgard 184, Dow Corning Inc., Midland, MI). The fabrication included five major steps: (1) SU-8 master fabrication, (2) PDMS casting, (3) surface printing of hydrophobic polymers such as Teflon on the glass substrate, (4) plasma bonding of PDMS to the glass substrate, (5) surface passivation with PLL-g-PEG solution. The master for the PDMS device was fabricated using standard photolithography techniques with SU-8 2015 photoresist (MicroChem, Newton, MA). The positive master mold for the device contained channels that were 10  $\mu\text{m}$  deep. In order to prevent adhesion with PDMS, the master mold was treated with hexamethyldisilane (Sigma-Aldrich, St. Louis, MO) for 1 hour. After the silane treatment, PDMS was poured onto the master mold, which was degassed in a desiccator with a ~5 psi vacuum for 30 minutes before pouring. After curing in an oven at 65°C for 3 hours, the PDMS layer was peeled from the silicon master. A metal syringe needle with an outer diameter of 1/16 inches (Hamilton

Company, Reno, NV) was used to punch holes through the end of the channels for connection with 1/16-in. Teflon tubing. It was treated with an oxygen plasma in a plasma cleaner (Harrick Plasma, Ithaca, NY) for 1 minute 40 sec. before it was bonded to the patterned glass substrate. To print a hydrophobic solution on the glass substrate, we used the micro flow patterning technique.<sup>15</sup> Using a reversibly bonded PDMS mold with two parallel zigzag microchannels (10 µm deep, 100 µm wide and 5 mm long channel, the clearance between each channel was 150 µm), we printed 1 µL Teflon solution (DuPont, Wilmington, DE) by flowing it through the microchannels. Negative pressure was applied at the end of the channel. After the channels were filled with Teflon, we peeled off the PDMS mold and cured the patterned Teflon structure on a hotplate at 100 °C for 10 sec. Then, we removed the excessive Teflon material around the reservoir holes and left only the channel sections on the glass slide. The thickness of the printed Teflon stripe was measured with WYKO NT 9800 Optical Surface Profiler (Veeco, Plainview, NY). To align the PDMS chip to the Teflon pattern on the glass substrate, we used a stereoscope (Olympus, SZX16).

### Surface treatment

After oxygen plasma bonding, poly(L-lysine)-grafted-poly(ethylene glycol) (or PLL-g-PEG) copolymers were applied to prevent non-specific binding on the PDMS device. This coating also helped to reduce the electroosmotic flow (EOF). The polycationic PLL backbone interacts with the negatively-charged surface and builds a monolayer.<sup>16</sup> A negative pressure was applied at the outlets of the sorting channel to fill the device with 1mM PLL-g-PEG solution. It was then incubated in the device for 15 min. and flushed out with DI water.

### Device Operation

The device was operated with pressure-driven flow. The sample entered through the middle inlet via an autosampler (1200 Series LC, Agilent, Wilmington, DE) and was hydrodynamically focused by two sheath flows. Two standard syringe pumps (Kent Scientific Corporation, Torrington, CT) were used for the sheath buffer solutions. For the strong electrolytes in the electrode channels, we continuously pumped 3M KCl into the two parallel electrode channels using a dual syringe pump (Harvard Apparatus, Holliston, MA). To adjust the flow rate of the strong electrolyte, so that the electrolyte did not cross over the printed junctions into the sorting channel, we added 1 µM FITC (fluorescein isothiocyanate) to the electrolyte and adjusted the flow rate between 0.5–1 µL/min. while observing the fluorescence signal of the electrolyte (see Figure S-1 of Supporting Information). At the end of each electrode channel, a Pt wire was placed slightly above the electrode channel outlets to apply an electric field across the sorting channel. In this way, the bubbles generated by the electrolysis remained outside of the KCl-filled electrode channels and had no effect on the electric field for the sorting process. To collect the fractionated samples, we inserted a 10 µL or 200 µL pipette tip into each outlet.

### Materials and Reagents

Eight IEF markers (Sigma-Aldrich, St. Louis, MO) with pI values of 4.5, 5.1, 5.5, 6.2, 6.6, 6.8, 7.2 and 9.0 and a concentration of 1µg/mL were used for this experiment. These IEF markers can be detected by fluorescence microscopy with an excitation wavelength from 330 to 340nm and an emission wavelength from 415 to 500 nm. For protein separations, recombinant green-fluorescent protein (GFP), with a molecular weight of 27-kDa and a pI value of 5.0 (Clontech, Palo Alto, CA), and R-Phycoerythrin, a high molecular weight protein (240-kDa) with a pI value of ~4.6 (Cyanotech, Kailua-Kona, HI), were used. The sample buffers were prepared by adding appropriate volumes of the mono- ( $\text{NaH}_2\text{PO}_4$ ) and dibasic sodium phosphate buffer ( $\text{Na}_2\text{HPO}_4$ ) and deionized water at different ratios to obtain a phosphate buffer at pH 5.5~8.0.<sup>17</sup> As a strong electrolyte, we used 3 M KCl. An inverted epi-fluorescence microscope

IX 51 (Olympus, Melville, NY), equipped with a thermoelectrically cooled CCD camera (Cooke Co., Auburn Hill, MI) was used for imaging. Sequences of images were taken and analyzed by the image-processing software ImagePro Plus (Media Cybernetics, Silver Spring, MD). The pH value of the sample was measured with a micro pH probe (Microelectrodes Inc., MI-413, NH) and adjusted with 10mM NaOH or 0.25% acetic acid. To validate the sorting results with mass spectrometry, we used 9 different synthetic peptides, as listed in Table S-1 of Supporting Information. As an example for sorting of complex sample mixtures, we tested a commercial standard tryptic digest of bovine serum albumin (BSA; Agilent, CO). The LC column used during MS was Agilent ZORBAX with a pore size of 3.5  $\mu\text{m}$  on an Agilent LC/MSD-TOF. The sorting and sample preparation steps for LC-MS analysis are shown in Figure S-2 of Supporting Information. For a sorting test of proteins, we used insulin (bovine, MW 5734.51), cytochrome C (equine, MW 12361.96), apomyoglobin (equine, MW 16952.27), and albumin (MW 66430.09), all from the ProteoMass peptide&protein MALDI-MS calibration kit (Sigma Aldrich, MO). For desalting of the fractionated samples for MALDI-MS, we used ZipTips (Milipore, Billerica, MA).

## RESULTS AND DISCUSSION

To meet the requirement of an efficient coupling of the electrical field while creating sufficient hydrodynamic resistance to the sample flow from the sorting channel, we have used a simple surface printing technique to generate junction gaps between the sorting channel and electrode channels on each side. This surface printing method is schematically shown in Figure 1. The pattern can consist of multiple parallel lines crossing the sorting channel or two zig-zag lines connecting the sorting channel and electrode channels on both sides. The surface-printed Teflon pattern with a thickness of ~500 nm on the glass substrate created controlled rupture points upon applying pressure-driven flow after plasma bonding between the PDMS cover and glass substrate. These rupture points, with possibly micron-size or smaller openings, acted as junction gaps between the sorting channel and electrode channels when applying electric field across the channels. Instead of integrating planar gold electrodes into the electrode channels, which requires e-beam deposition of the electrodes onto the glass substrate, and alignment before bonding to the PDMS cover, we filled the electrode channels with a highly conductive solution such as 3M KCl at a flow rate of 0.5–1  $\mu\text{L}/\text{min}$ , using a syringe pump, and placed a Pt wire directly above each outlet reservoir to achieve an electrical connection to the sorting channel.

In Figure 2a, the schematic of the single-step sorting process is shown. At a given pH of the buffer solution, the middle outlet collects molecules with their pI values close to the pH value of the buffer solution. The collectable pI range of this “isoelectric trap” can be adjusted with the width of the middle outlet channel as well as with the length of the sorting channel, depending on the flow speed. Molecules with higher electrophoretic mobilities are deflected to either side away from the middle outlet channel and can be collected either from the left or right outlet channels depending on the polarity of their charge (negative to the anode and positive to the cathode). In this way, we sort the entire molecules into three groups (neutral, higher or lower pI values than the buffer pH). Even though the free-flow zone electrophoresis process is based on the charge to mass ratio, we don't differentiate between molecules with different masses in our sorting/collecting scheme, but only differentiate between the positive and negatively charged species. All fractionated samples are collected with standard 10  $\mu\text{L}$  or 200  $\mu\text{L}$  pipette tips. A single sorting device in PDMS is shown in Figure 2b along with the surface-printed hydrophobic Teflon stripes inside the device in Figure 2c. The sorting channel was 2 mm wide, 5 mm long and 10  $\mu\text{m}$  deep. The three outlets allowed collecting the positively and negatively charged samples that could be further fractionated to decrease the sample complexity for

subsequent analysis. We confirmed the functionality of the device with a positive (Rhodamine 123, 2.5 μM) and negative dye (FITC, 1μM) in Figure 2d. The direction of the deflection was in accordance with the polarity of the dye.

We characterized the surface-printed junction with the I–V measurement (see Figure S-3 of Supporting Information). The total current across the junction was the lowest with  $I_{total} = 10 \mu\text{A}$  at  $V_{applied} = 210 \text{ V}$  when the device was filled with the 3M KCl solution in the electrolyte channel and with 5 mM phosphate buffer solution in the sorting channel by capillary force without using a syringe pump ( $Q_{KCl} = 0 \mu\text{L}/\text{min}$ ). When applying a positive pressure on the electrode channel at a flow rate of  $Q_{KCl} = 0.5 \mu\text{L}/\text{min}$ , the total current increased to  $I_{total} = 81 \mu\text{A}$  at  $V_{applied} = 210 \text{ V}$ . At  $Q_{KCl} = 0.75 \mu\text{L}/\text{min}$ , the total current even increased to  $I_{total} = 115 \mu\text{A}$  at 210V. This result demonstrates that we can tune the gap size of the junction by increasing the flow rate of the electrolyte solution. This tunability of the junction size is enabled by the flexible nature of the PDMS material. The total resistance of the sorting device  $R_{total}$  can be calculated as follows:

$$R_{total}=2R_{junction}+R_{sorting}+2R_{electrode} \quad (1)$$

, whereby  $R_{junction}$  is the resistance of the surface-printed junction on each side,  $R_{sorting}$  is the resistance of the sorting channel, and  $R_{electrode}$  is the resistance of the electrode channel (see the calculation of each resistance value in Supporting Information). Therefore, the resistance of the junction on each side can be calculated according to eqn. 1) as follows:

$$\begin{aligned} R_{junction} &= \frac{R_{total} - R_{sorting} - 2R_{electrode}}{2} \\ &= \frac{2M\Omega - 620k\Omega - 2 \cdot 129k\Omega}{2} = 561k\Omega \end{aligned} \quad (2)$$

Using this resistance value  $R_{junction} = 561\text{k}\Omega$ , we calculated the potential loss at  $V_{applied} = 200\text{V}$  across the junction on each side as follows ( $I_{total} = 100\mu\text{A}$  at 200V, see the I–V curve at 0.75 μL/min. in Figure S-3 of Supporting Information):

$$\begin{aligned} V_{junction} &= I_{total} \cdot 2R_{junction} \\ &= 100\mu\text{A} \cdot 2 \cdot 561\text{k}\Omega = 112.2\text{V} \end{aligned} \quad (3)$$

The potential drop in the electrolyte channel was relatively low due to the high electric conductivity of the 3M KCl solution:

$$\begin{aligned} V_{electrode} &= I_{total} \cdot 2R_{electrode} \\ &= 100\mu\text{A} \cdot 2 \cdot 129\text{k}\Omega = 25.8\text{V} \end{aligned} \quad (4)$$

For our sorting process, the effective potential across the sorting channel was  $V_{effective} = 62\text{V}$  when  $V_{applied} = 200\text{V}$  was applied. This result means that 31% of the applied potential can be coupled through the junction into the sorting process. The effective electric field across the 2mm wide sorting channel was  $E_{effective} = V_{effective}/L_s = 62\text{V}/0.2\text{cm} = 310\text{V/cm}$  accordingly. With this resistance value, we estimated the gap size of 24 individual subjunctions to be ~698nm assuming that the junction is of rectangular shape and filled with 3M KCl solution (see the calculation of the junction gap size in Supporting Information). This estimated gap size of the junction corresponds approximately to the thickness of the printed Teflon on the glass substrate which is ~500nm. At  $Q_{KCl} = 0 \mu\text{L}/\text{min}$ , the corresponding gap size is ~41nm.

As for the reproducibility between sorting chips, the CV value was calculated, as shown in Figure S-5 of Supporting Information. The average CV value was 12.5% at  $Q_{KCl} = 0.5 \mu\text{L}/\text{min}$ . which means an acceptable reproducibility between chips. In the case of  $Q_{KCl} = 0.75 \mu\text{L}/\text{min}$ , even though we could couple higher electric field into the sorting process, the CV value increased to 27% which means that a calibration prior to the sorting process is required to set the voltage required for the sorting process. Compared to our previous diffusion-potential-driven pI-based sorting<sup>18</sup>, we could apply a 15-fold higher electrical field across the sorting channel.

To evaluate the sorting capability of the device, we used three fluorescent pI markers, pI 10.3, 8.7 and 6.6, in 20 mM phosphate buffer at pH 8.4. As shown in Figure 3a, three bands were clearly visible in the presence of an electric field of  $E = 310 \text{ V/cm}$  in the sorting channel. The positively charged pI marker 10.3 was focused toward the cathode (left) while the negatively charged pI marker 6.6 was focused to the anode (right). pI marker 8.7 with its pI value close to pH 8.4 was collected from the middle outlet. With a mixture of 5 different pI markers, five streams could be detected (Figure 3b). Among them, the separation between pI 5.1 and 4.5 implied that a separation resolution of  $\sim 0.5 \text{ pI}$  units was achievable with this device. This result suggests that we can sort the peptides based on the charge at a given pH value of the buffer solution. Each sorting outlet seemed to correspond to a specific pI value. However, there will be examples where this trend that correlated to pI might not hold, especially in cases where the pI is very different from the buffer pH. In this study, however, the primary objective of this device was to separate positively charged species (presumably pI values higher than pH of the buffer) from negatively charged species (pI values lower than pH values). Separation between negative species (or positive species) was not critical in actual implementation of this device as a sample preparation tool. We also showed that a volatile buffer such as ammonium acetate can be used for our pI-based sorting process as an alternative to phosphate. As shown in Figure 3c, three pI markers, pI 9.0, 7.2 and 5.1, were successfully separated in 20 mM ammonium acetate at pH 7 with an electrical field of  $E = 279 \text{ V/cm}$ . This result implied that a direct MS integration of the fractionated samples from the device could be possible without a desalting step. We also separated two different proteins, GFP and R-Phycoerythrin, differing by only 0.5 pI units into two streams (Figure 3d). This demonstrated the high-throughput capability of the device by processing raw samples at a flow rate of up to  $1 \mu\text{L}/\text{min}$ , which is sufficient for downstream, standard biomolecule assays such as MS. Although it was our aim here to perform only a binary sorting, namely a sorting of the mixture into a group of positively charged molecules and a group of negatively charged molecules, the sorting device with several outlets such as the device with 11 outlets in Figure 3 could fractionate the samples into several subfractions among positively and negatively charged species to obtain less complex samples.

To validate the sorting result with MS, we fractionated a test mixture of 8 synthetic peptides, pI 9.7, 8.8, 6.8, 6.7, 6.3, 6.1, 5.1, 3.6 (Figure 4), into three pI groups at pH 7.0. From the cathodic side ( $\text{pI} > \text{pH } 7.0$ ), we could collect the basic peptides ( $\text{pI } 9.7$  and 8.8). From the middle outlet acting as the isoelectric trap ( $\text{pI} \sim \text{pH } 7.0$ ), we collected those peptides with pI values close to pH 7.0 such as pI 6.8 and 6.7. These two peptides, 6.8 and 6.7, were also found along with more acidic peptides such as pI 6.3, 6.1, 5.1, and 3.6 in the anodic sample. Especially, in the case of the peptide pI 5.1, higher signal intensity was detected after removing basic peptides.

By coupling two sorting steps at two different pH values via pH titration, we can isolate the peptides within a specific pI range set by the pH difference which would be extremely useful for targeted proteomics. To demonstrate such an isolation of the peptides within specific pI range through two coupled, cascaded sorting steps, we mixed 5 different peptides (pI 8.8, 6.8, 6.7, 6.3, 3.6) and isolated those peptides between pI 6–7 out of the mixture by sequentially sorting the sample at pH 7 and 6. The schematic of the two-step sorting is shown in Figure 5a. To quantify the sample loss, we added an internal standard peptide with known mass and

concentration (MW 1013.6, pI 6.9) to each fractionated sample before MS analysis and used its signal intensity as an internal reference standard. We normalized the signal intensity of each peptide relative to that of the internal standard peptide before and after sorting and calculated the signal intensity ratio  $\eta$ . The result of this two-step sorting experiment for the peptide mixture with three separate runs is shown in Figure 5b. We could identify the basic peptide with pI 8.8 from the cathodic sorting channel while the peptides with pI values close to the buffer pH value of pH 7, pI 6.8 and 6.7, were collected from the middle sorting channel. In the case of pI 8.8, we observed as much as a two-fold increase of the signal intensity ratio  $\eta$  after the sorting step, due perhaps to an increase in the ionization efficiency of this peptide after removing acidic peptides from the mixture. After collecting the acidic peptides from the anodic sorting channel and running the second sorting step at a lower pH value, pH 6, we could isolate pI 6.8 and pI 6.7, switched into the positive charge state at pH 6, from the cathodic sorting channel while the negatively charged peptide at pH 6, pI 3.6, was collected through the anodic sorting channel. However, peptide pI 6.3, with a pI value close to the pH value of the buffer solution, was collected from the middle outlet instead of from the cathodic sorting channel. This result showed that a pH difference less than 0.5 pH units was not sufficient for free-flow zone electrophoresis sorting of the peptides in our device. In the second sorting step, the sample loss for pI 6.8 (sample recovery rate of 28%) and pI 6.7 (sample recovery rate of 17.3%) was mainly caused by sorting out these two peptides through the middle outlet in the first sorting step and not using them again in the second sorting step. The sample loss may have also been caused partly by the vacuum centrifugation process in the SpeedVac machine when concentrating the diluted samples after the first sorting step. This result validated the concept that two fractionation steps can be coupled via off-chip titration and enables isolating peptides within a predetermined pI range set by the pH values of the buffers. The currently collectable pI range is  $\sim 1$  pH units. However, by further optimizing the device geometry such as channel length and width and improving the membrane between the sorting and electrode channels, we may be able to isolate peptides within lower pI range such as  $\sim 0.5$  pH units. One possible solution to minimize the sample loss would be an on-line coupling of two steps on a single chip with on-chip pH titration.

We applied this sorting technique to more complex peptide samples such as a BSA tryptic digest. In Figure 6, the single-step sorting result of the tryptic digest BSA at pH 7 is shown. From the 15 identified peptides of the tryptic digest BSA sample, we could sort out all the highly basic peptides that would be difficult to isolate with conventional gel-based separation techniques. In addition, we could detect the peptide with MW 403.23 and pI 10.1 which was not detected before sorting. The lowest signal ratio of before and after sorting was 45% in case of the peptide with MW 431.27, while the peptides with MW 688.36 and MW 732.41 showed an increase of the signal intensity up to 149% after sorting. In case of the acidic peptides, we observed a decrease of the signal intensity for those peptides with their pI values close to pH 7 of the buffer solution since some of them were partially sorted out to the middle outlet and were not used for MS analysis. However, peptide with MW 921.48 showed a 225% increase of the signal intensity. Furthermore, we could detect two highly acidic peptides (MW 885.4 and MW 1566.7) which were not detected before sorting, but became detectable after the sorting step. These peptides were presumably undetected in the original peptide mixture because of ion-suppression by other highly abundant peptides. This result clearly shows that the single-step sorting strategy works for complex mixtures, and enables detection of more peptides after sorting step. Especially, the highly basic peptides with pH values above 10 could be successfully collected and identified with LC/MS. The MS spectra of the fractionated basic peptides collected from the cathodic outlet of the microfluidic sorting device is shown Figure S-6 of Supporting Information. Among the fractionated acidic peptides, highly acidic ones with a pI value of 3.6 and 4.1 could be detected after pI-based sorting (see MS spectra of the acidic peptides in Figure S-7 of Supporting Information). After the second sorting step at pH 6, however, we observed a significant sample loss for the peptides in the pI range 6–7 (pI 6.4,

6.7 and 6.8) above 90%. We are currently working on the improvement of the sorting process in order to reduce the sample loss after the second sorting step. We believe that we can solve this problem by coupling two sorting steps on a single chip.

We also tested the microfluidic sorting chip with a mixture of proteins and validated the sorting result with MALDI-MS. We have tested a mixture of 4 different proteins and could fractionate it into acidic and basic proteins at pH 7, as shown in Figure 7. This fractionation reduced the sample complexity and simultaneously enhanced the detection sensitivity for molecules with low signal intensity, as shown with the albumin in Figure 7b. From the acidic outlet, we could collect the acidic proteins such as albumin with single and double charges (pI 5.6), as well as insulin with pI 6.9. In the fraction from the middle outlet, we sorted out insulin and apomyoglobin with pI 7.2. In the same fraction, cytochrome C could be also detected. From the cathodic side, we could sort out cytochrome C with pI 9.6. In summary, we have demonstrated free-flow zone electrophoresis-based sorting of peptides as well as of proteins. By coupling two sorting steps off-line via pH titration, we isolated peptides within a specific pI range ( $\leq 1.0$  pH units) from the mixture. The pI range was determined simply by changing the buffer pH.

## CONCLUSIONS

We have developed a continuous-flow and ampholyte-free microfluidic sorting device based on free-flow zone electrophoresis. Since there is no need for specialized buffers or carrier ampholytes, coupling to downstream analyses such as LC-MS is facilitated. To couple an electric field into the sorting process, we printed a thin Teflon layer on top of the glass substrate and plasma bonded the PDMS channel to the printed glass substrate. Since the plasma bonding occurs only at the non-printed areas, the Teflon pattern created salt bridges between the sorting and electrode channels with an electric field coupling efficiency of 31%. The measurement of fluorescent molecules suggests that the sorting resolution can be as high as  $\sim 0.5$  pH units, which is sufficient for sample preparation applications. Because separation is performed in a continuous flow with a typical flow rate between  $0.5\text{--}1\mu\text{L}/\text{min}$ , this method enables high throughput sample preparation. We validated the sorting result with LC-MS and quantified the sample loss after each sorting step in the case of the synthetic peptides. We also coupled two sorting steps via off-line titration and isolated peptides within 1 pH units out of the synthetic peptide mixture. In addition, we demonstrated a single-step sorting for more complex samples such as BSA tryptic digest and for proteins. The main advantage of our sorting scheme is that the pI range of fractionation can be adjusted simply by programming buffer pH values, without any restriction on the buffers used. In addition, the operation could be extended to very high (even above pH 10) or low pH (below pH 3), as long as the buffer pH could be titrated to the values desired. Moreover, the continuous-flow sorting occurs mainly in a free solution, enabling a high sample throughput with minimal loss and bias caused by target-capturing membranes/columns/gels. However, the off-chip coupling created a high sample loss that makes an on-chip coupling between two sorting steps via on-chip pH titration necessary. Also, we have to reduce the amount of peptides lost to the isoelectric trap (middle channel outlet) to increase the sample recovery rate. We believe that, once further developed, this device will have significant impact on bioanalysis, especially for MS-based methods. This device enabling two sorting steps could be used as a generic prefractionation tool for isolating narrow pI range ( $\leq 0.5$  pH units) target molecules from complex protein samples or global peptide digests in targeted proteomics.

## Supplementary Material

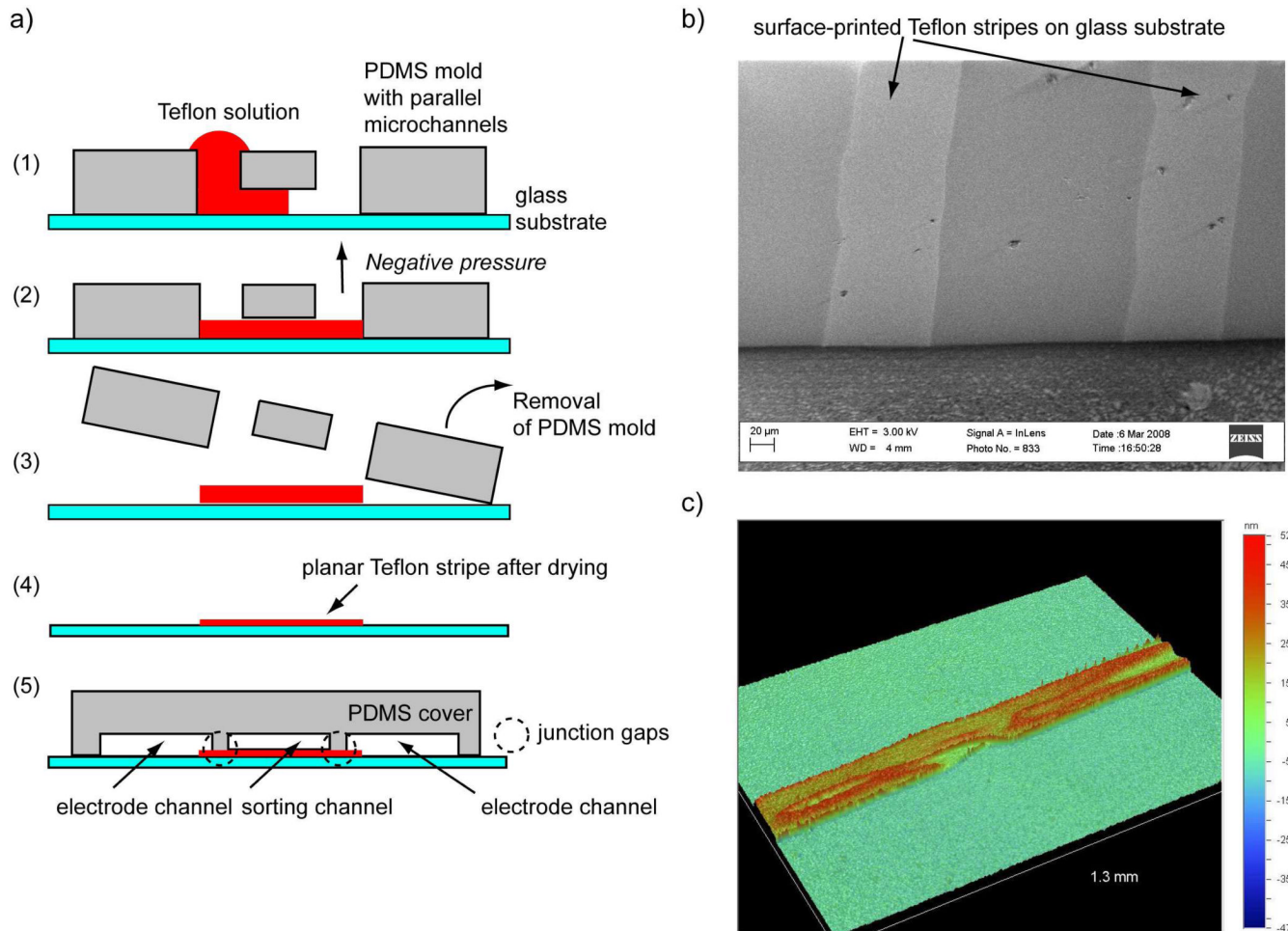
Refer to Web version on PubMed Central for supplementary material.

## Acknowledgments

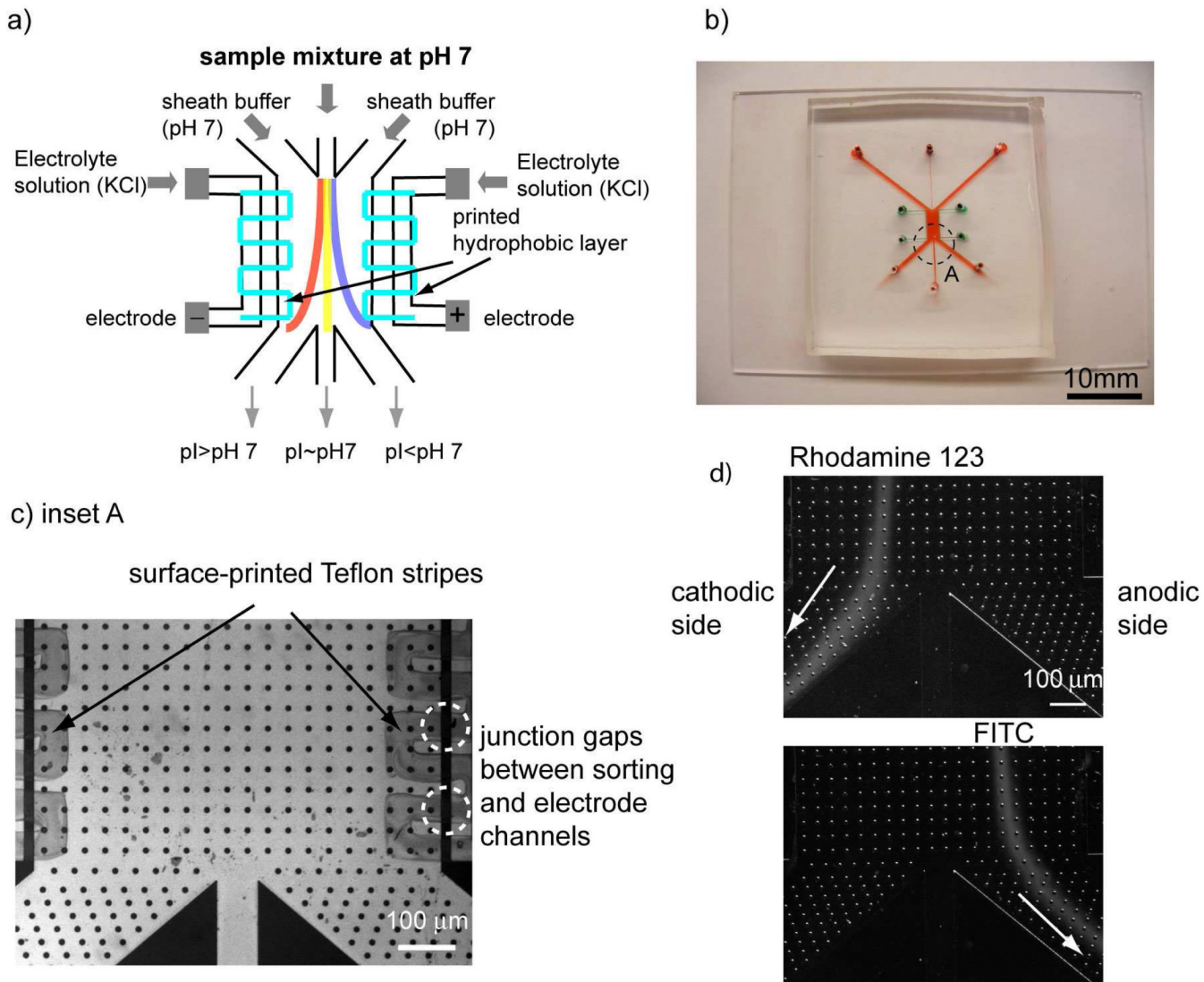
This work was partially supported by KIST-Intelligent Microsystems Center of Korea, MIT Center for Environmental Health Sciences (NIEHS Grant No. P30-ES002109), and NIH R21 EB008177. We thank the Tannenbaum Group at MIT for their help in MS analyses and discussions.

## REFERENCES

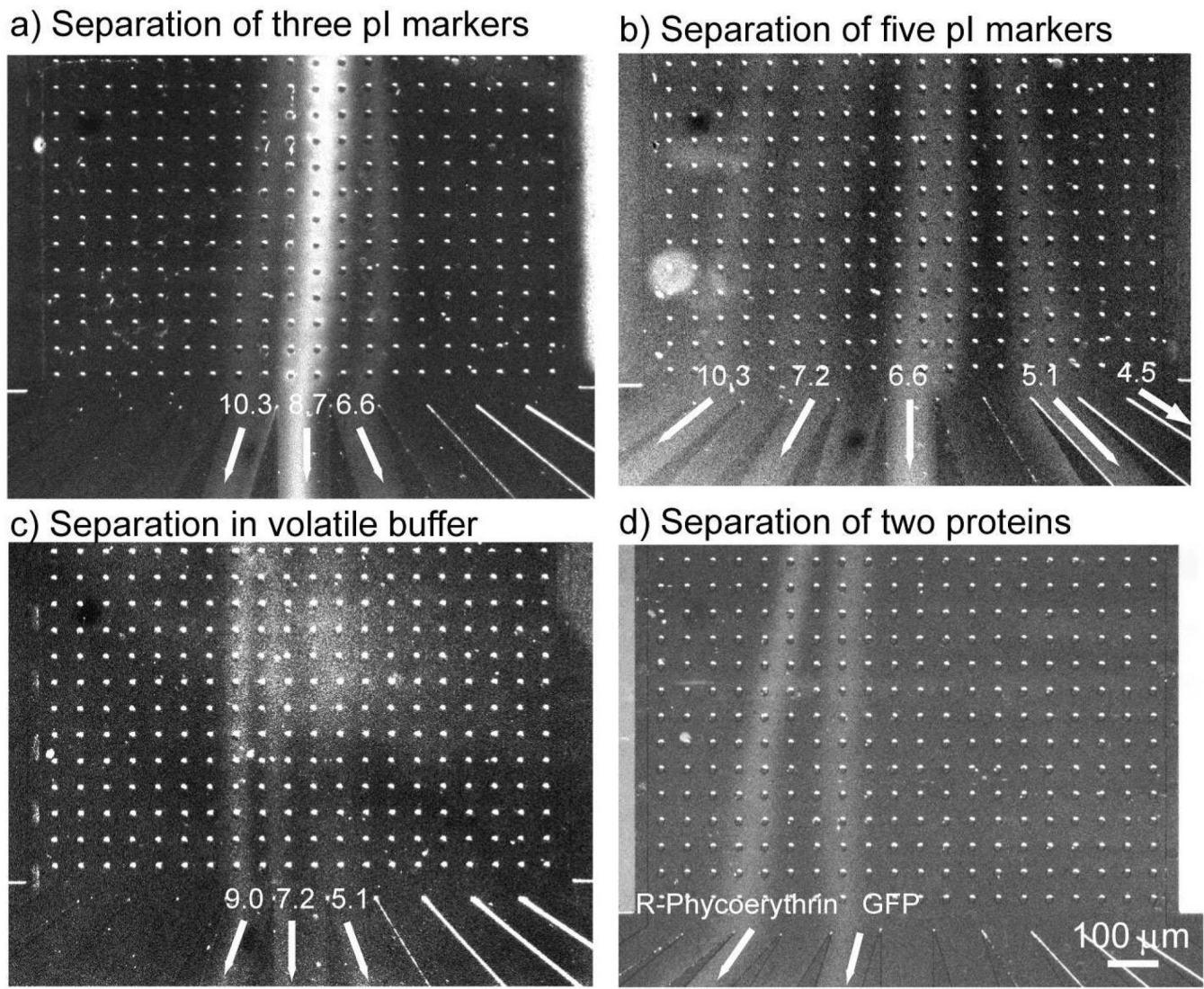
1. Washburn MP, Wolters D, Yates JR III. *Nat. Biotechnol* 2001;19:242–247. [PubMed: 11231557]
2. Wolters DA, Washburn MP, Yates JR III. *Anal. Chem* 2001;73:5683–5690. [PubMed: 11774908]
3. Immel D, Greven S, Reinemer P. *Proteomics* 2006;6:2947–2958. [PubMed: 16619308]
4. Pamme N. *Lab Chip* 2007;7:1644–1659. [PubMed: 18030382]
5. Kohlheyer D, Eijkel JCT, van den Berg A, Schasfoort RB. *Electrophoresis* 2008;29:977–993. [PubMed: 18232029]
6. Zhang CX, Manz A. *Anal. Chem* 2003;75:5759–5766. [PubMed: 14588015]
7. Kohlheyer D, Besselink G, Schlautmann S, Schasfoort RB. *Lab Chip* 2006;6:374–380. [PubMed: 16511620]
8. Kohlheyer D, Eijkel JC, Schlautmann S, van den Berg A, Schasfoort BM. *Anal. Chem* 2007;79:8190–8198. [PubMed: 17902700]
9. Albrecht J, Jensen K. *Electrophoresis* 2006;27:4960–4969. [PubMed: 17117380]
10. Albrecht J, El-Ali J, Jensen K. *Anal. Chem* 2007;79:9364–9371. [PubMed: 17994708]
11. Janasek D, Schilling M, Manz A, Franzke J. *Lab Chip* 2006;6:710–713. [PubMed: 16738720]
12. Fonslow B, Bowser M. *Anal. Chem* 2005;77:5706–5710. [PubMed: 16131085]
13. Fonslow B, Barocas V, Bowser M. *Anal. Chem* 2006;78:5369–5374. [PubMed: 16878871]
14. Song, YA.; Han, J.  $\mu$  TAS. Locascio, LE.; Gaitan, M.; Paegel, BM.; Ross, D.; Vreeland, WN., editors. Vol. Vol. 2. San Diego: 2008. p. 1323–1225.
15. Lee JH, Song YA, Han J. *Lab Chip* 2008;8:596–601. [PubMed: 18369515]
16. Ruiz-Taylor LA, Martin TL, Zaugg FG, Witte K, Indermuhle P, Nock S, Wagner P. *PNAS* 2001;98:852–857. [PubMed: 11158560]
17. Deutscher, MP. Guide to Protein Purification. Academic Press; 1990.
18. Song YA, Hsu S, Stevens A, Han J. *Anal. Chem* 2006;78:3528–3536. [PubMed: 16737204]

**Figure 1.**

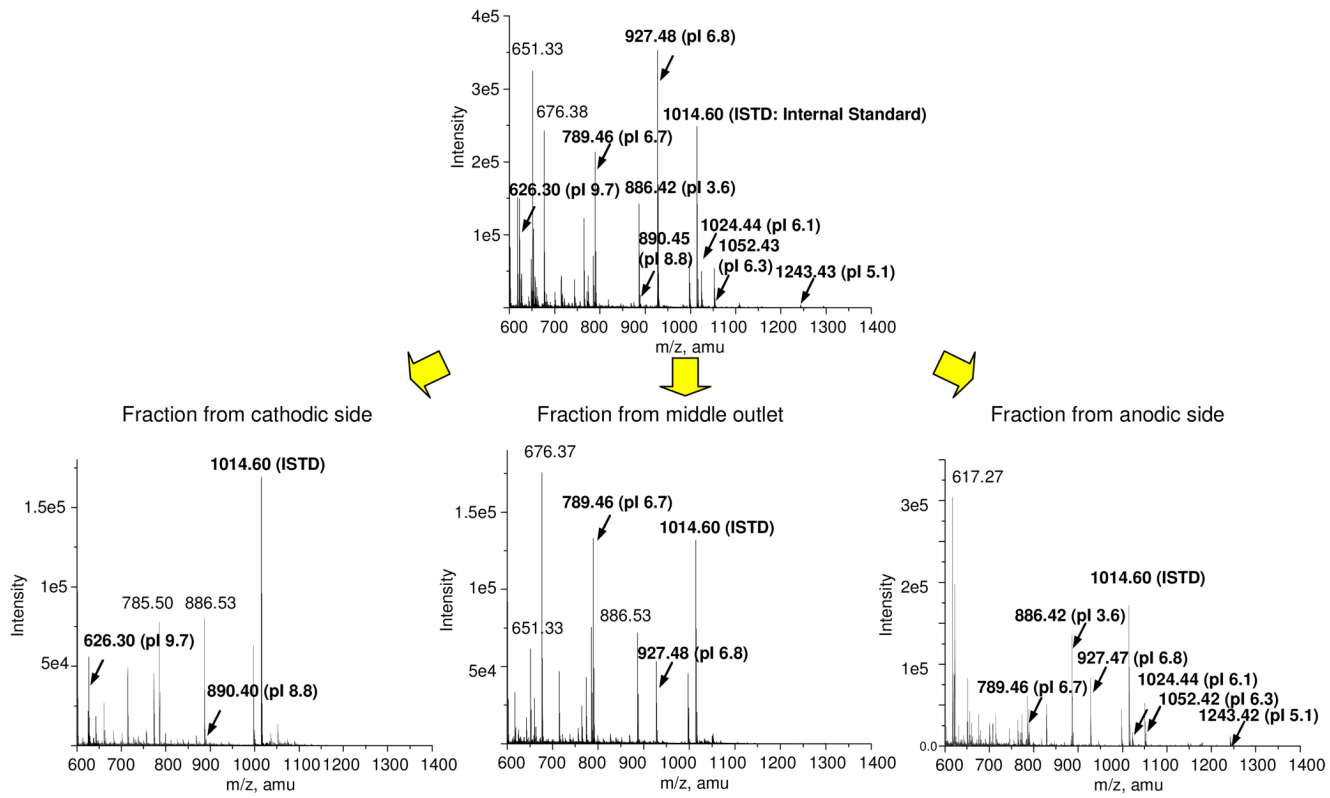
a) Fabrication scheme of the PDMS pi-based sorting device: 1) filling of a reversibly bonded PDMS microchannel with Teflon solution, 2) applying negative pressure to flush the Teflon solution through the microchannel completely, 3) removal of the PDMS mold, 4) curing of the Teflon film on a hotplate at 70°C for 5 min., 5) oxygen plasma bonding of the PDMS cover on top of the printed glass substrate. b) SEM image of the surface- printed Teflon stripes on a glass substrate. Teflon stripes generate multiple junction gaps between the channels of the plasma-bonded PDMS cover, c) Surface profile of a single Teflon stripe. The maximum stripe thickness was ~500 nm.

**Figure 2.**

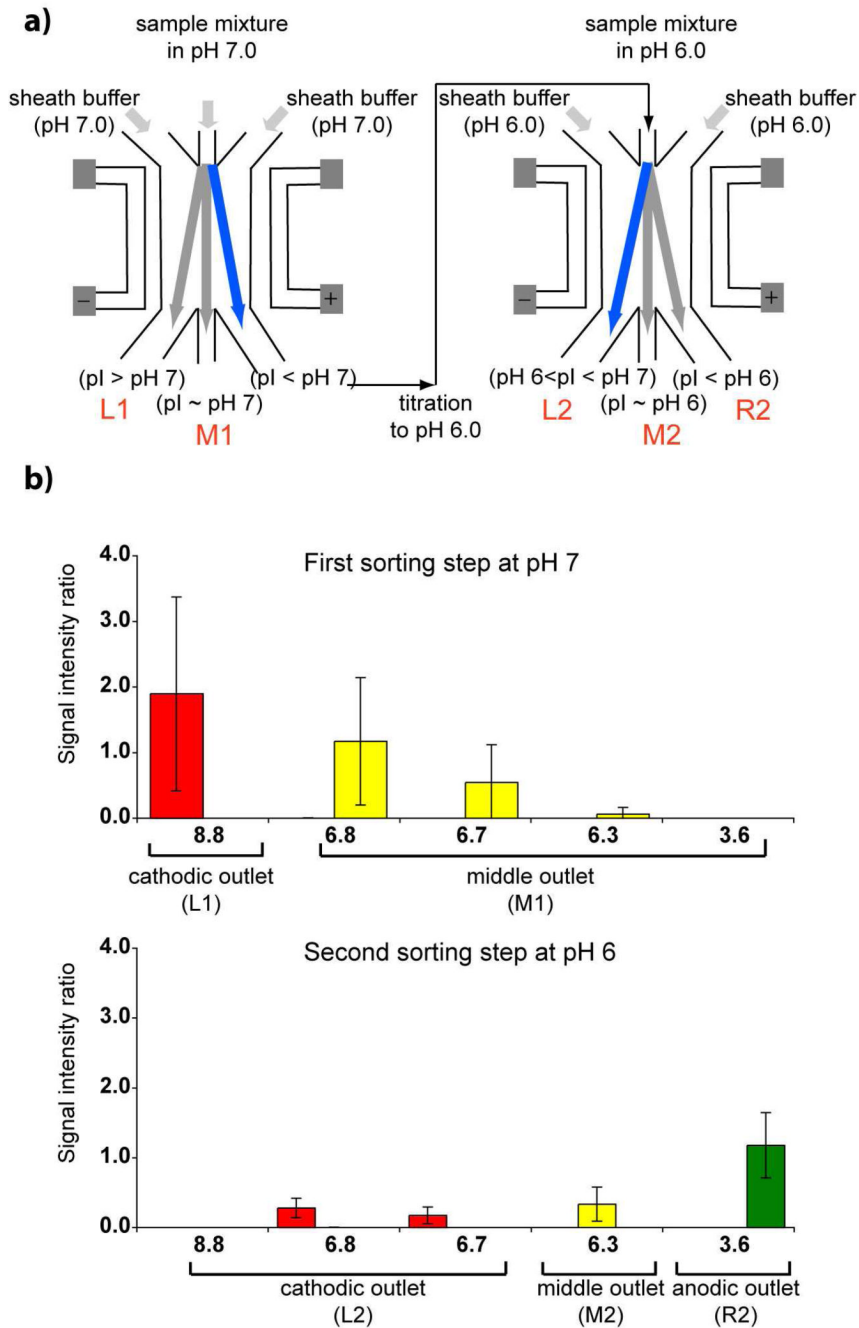
a) Schematic of the pI-based sorting device. The sample is injected from the autosampler into the middle inlet. The width of the sample flow can be varied by adjusting the flow rates of the sheath buffer solutions. On each side, there is an electrode channel running parallel to the main sorting channel. It is filled with 3 Mol KCl solution. The distance between the side and main channel is 50  $\mu$ m. b) pI-based sorting device in PDMS with 3 outlets. The number of the outlets can be increased depending on the desired number of fractionated samples (a device with 11 outlets is shown in Figure 3) c) printed Teflon stripes inside the device generate gap junctions acting as salt bridges. The sorting channel was 2 mm wide, 5 mm long and 10  $\mu$ m deep. d) Sorting test with a positive (Rhodamine 123) and negative dye (FITC) at 150V and  $\sim$ 300  $\mu$ A across the sorting channel. According to the polarity of the molecular charge, the direction of deflection was determined by using two different filters (488 nm, 570 nm).

**Figure 3.**

a) Separation of three pI markers (pI 10.3, 8.7 and 6.6) in 10mM phosphate buffer at pH 8.4,  $E = 310 \text{ V/cm}$ , sample flow rate of  $1 \mu\text{L}/\text{min}$  and buffer flow rate of  $2.5 \mu\text{L}/\text{min}$ . b) Separation of five pI markers (10.3, 7.2, 6.6, 5.1, and 4.5 from left to right) in 10mM phosphate at pH 6.0,  $E = 310 \text{ V/cm}$ , sample flow rate of  $1 \mu\text{L}/\text{min}$  and buffer flow rate of  $2.5 \mu\text{L}/\text{min}$ . c) pI markers 9.0, 7.2 and 5.1 in 20mM ammonium acetate with pH 7.0,  $E = 279 \text{ V/cm}$  and sample flow rate of  $0.5 \mu\text{L}/\text{min}$  and buffer flow rate of  $2.0 \mu\text{L}/\text{min}$ . d) separation of GFP (pI 4.8) and R-phycoerythrin (pI 4.3) in 10 mM phosphate at pH 6.0,  $E = 310 \text{ V/cm}$  and sample flow rate of  $0.5 \mu\text{L}/\text{min}$  and buffer flow rate of  $2.0 \mu\text{L}/\text{min}$ . Both proteins were negatively charged at pH 6.0 and therefore, deflected to the anodic side. Although R-Phycoerythrin has a higher MW (240kDa versus 27kDa), it deflected more to the side than GFP due to its higher charge (pI 4.3 versus pI 4.8). This fluorescence image clearly demonstrates that it is possible to perform a sorting of the proteins within 0.5 pI units using our pI-based sorter.

**Figure 4.**

ESI-MS result of a single fractionation of 8 peptides (40 nM) at pH 7.0 with  $E = 279 \text{ V/cm}$  and  $0.5\mu\text{L/min}$ : a) peptide mixture before sorting (MW 625.74, pI 9.7; MW 889.38, pI 8.8; MW 926.47, pI 6.8; MW 788.45, pI 6.7; MW 1052.19, pI 6.3; MW 1023.43, pI 6.1; MW 1243.23, pI 5.1; MW 885.92, pI 3.6) with MW 1013.6 (pI 6.9) used as an internal standard peptide, b) basic peptides such as pI 9.7 and 8.8 were sorted out from the cathodic side, c) peptides with pI values close to pH 7.0, pI 6.7 and 6.8 were collected from the middle channel, d) acidic peptides, pI 3.6, 5.1, 6.1, 6.3, 6.7 and 6.8, were collected from the anodic side.

**Figure 5.**

a) Schematic of the two cascaded sorting steps to isolate the molecules within a specific pI range determined by the pH difference of the buffer solutions. (L1 and M1: cathodic fraction and fraction from the middle outlet after the first sorting step. L2, M2 and R2: cathodic fraction, fraction from the middle outlet, anodic fraction after the second sorting step) b) Quantification of the sample loss for each peptide fraction in the two-step sorting process after the first fractionation at pH 7.0 and the second fractionation at pH 6.0. As for the test peptide mixture, we used peptides with pI 8.8, 6.8, 6.7, 6.3 and 3.6.

## Before sorting

MW	pI value	TIC
<b>403.23</b>	<b>10.1</b>	<b>not detected</b>
431.27	11	2.64E+05
507.24	7	1.10E+06
536.27	10.1	1.20E+05
544.33	11	1.06E+06
688.36	11	2.55E+05
732.41	11	8.95E+05
788.46	6.7	7.86E+05
<b>885.4</b>	<b>3.6</b>	<b>not detected</b>
921.48	4.3	5.57E+05
926.49	6.8	5.36E+05
1162.63	4.3	3.53E+05
1304.71	5.2	6.16E+05
<b>1566.7</b>	<b>4.1</b>	<b>not detected</b>
1880.9	6.4	2.50E+05

## After sorting

The diagram illustrates the sorting process. A large bracket on the left groups all peptides from the 'Before sorting' table. Two arrows point from this bracket to two separate tables on the right. The top arrow, labeled 'Basic peptides from cathodic side', points to a table containing peptides with pI values of 10.1, 11, or 7. The bottom arrow, labeled 'Acidic peptides from anodic side', points to a table containing peptides with pI values of 4.3, 6.8, 6.7, or 4.1. The original table also includes MW and TIC values.

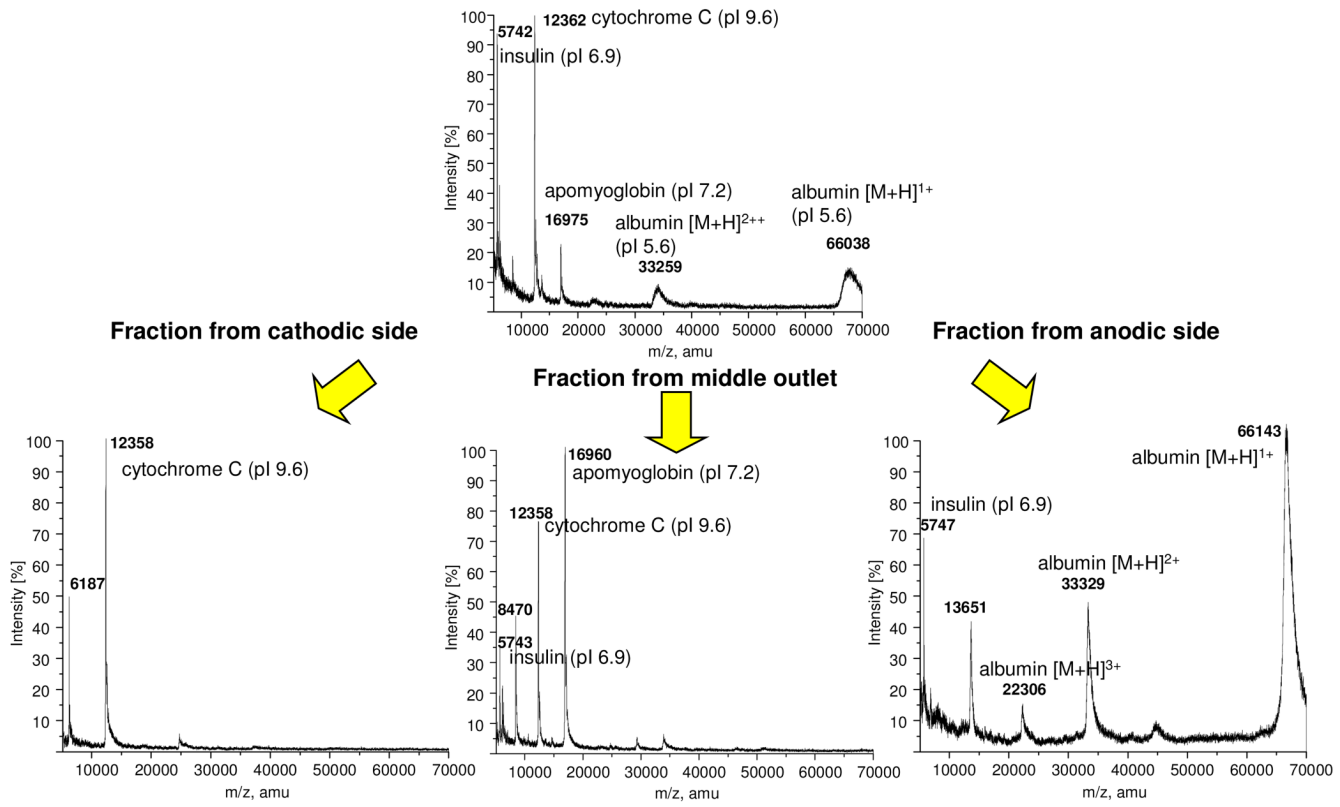
MW	pI value	TIC	signal ratio
<b>403.23</b>	<b>10.1</b>	<b>5.72E+04</b>	
431.27	11	1.19E+05	0.45
536.27	10.1	9.09E+04	0.76
544.33	11	8.99E+05	0.85
688.36	11	2.65E+05	1.04
732.41	11	1.33E+06	1.49

MW	pI value	TIC	signal ratio
507.24	7	2.42E+05	0.22
788.46	6.7	1.43E+05	0.18
<b>885.4</b>	<b>3.6</b>	<b>5.62E+04</b>	
921.48	4.3	1.25E+06	2.25
926.49	6.8	2.10E+05	0.39
1162.63	4.3	1.98E+05	0.56
1304.71	5.2	4.44E+05	0.72
<b>1566.7</b>	<b>4.1</b>	<b>5.71E+04</b>	
1880.9	6.4	8.92E+04	0.36

**Figure 6.**

Tryptic digest BSA standard before and after a single-step sorting at pH 7 into basic and acidic peptides.

**Figure 7.**

MALDI-MS result for a single fractionation of 4 different proteins (100 pmole/ $\mu$ L) with E = 279 V/cm at pH 7. a) mixture of insulin (bovine, MW 5734.51, pI 6.9), cytochrome c (equine, MW 12361.96, pI 9.6), apomyoglobin (equine, MW 16952.27, pI 7.2), and albumin (MW 66430.09, pI 5.6). b) acidic proteins, albumin and insulin, were collected from the anodic side. c) proteins with pI values close to pH 7.0 such as apomyoglobin and insulin were collected from the middle outlet. However, some contamination through cytochrome C can be also seen in the middle channel. d) basic protein, cytochrome C, was collected from the cathodic side.